JOURNAL OF VIROLOGY, Mar. 1990, p. 1050–1056
0022-538X/90/031050-07$02.00/0
Copyright © 1990, American Society for Microbiology
Vol. 64, No. 3

Coronavirus Transcription: Subgenomic Mouse Hepatitis Virus Replicative Intermediates Function in RNA Synthesis

STANLEY G. SAWICKI* AND DOROTHEA L. SAWICKI
Department of Microbiology, Medical College of Ohio, Toledo, Ohio 43699

Received 26 September 1989/Accepted 30 November 1989

Both genomic and subgenomic replicative intermediates (RIs) and replicative-form (RF) structures were found in 17CL1 mouse cells that had been infected with the A59 strain of mouse hepatitis virus (MHV), a prototypic coronavirus. Seven species of RNase-resistant RF RNAs, whose sizes were consistent with the fact that each was derived from an RI that was engaged in the synthesis of one of the seven MHV positive-strand RNAs, were produced by treatment with RNase A. Because the radiolabeling of the seven RF RNAs was proportional to that of the corresponding seven positive-strand RNAs, the relative rate of synthesis of each of the MHV positive-strand RNAs may be controlled by the relative number of each of the size classes of RIs that are produced. In contrast to alphavirus, which produced its subgenome-length RF RNAs from genome-length RIs, MHV RF RNAs were derived from genome- and subgenome-length RIs. Only the three largest MHV RF RNAs (RF_I, RF_{II}, and RF_{III}) were derived from the RIs that migrated slowest on agarose gels. The four smallest RF RNAs (RF_{IV}, RF_V, RF_{VI}, and RF_{VII}) were derived from RIs that migrated in a broad region of the gel that extended from the position of 28S rRNA to the position of the viral single-stranded MHV mRNA-3. Because all seven RIs were labeled during very short pulses with [^{3}H]uridine, we concluded that the subgenome-length RIs are transcriptionally active. These findings, with the recent report of the presence of subgenome-length negative-strand RNAs in cells infected with porcine transmissible gastroenteritis virus (P. B. Sethna, S.-L. Hung, and D. A. Brian, Proc. Natl. Acad. Sci. USA 86:5626–5630, 1989), strongly suggest that coronaviruses utilize a novel replication strategy that employs the synthesis of subgenomic negative strands to produce subgenomic mRNAs.

Coronaviruses are enveloped positive-strand RNA viruses that cause the production of subgenomic mRNAs that are 3′ coterminal with the genomic RNA; i.e., they comprise a nested set of mRNAs. Depending on the type or strain of coronavirus, five to seven subgenomic mRNAs are produced during infection. Each mRNA possesses an approximately 70-nucleotide-long sequence (referred to as the leader RNA) at its 5′ end that is also present at the 5′ end of the genome (for reviews, see references 12 and 23). Until recently, it was thought that coronaviruses generated their subgenomic mRNAs from a genome-length negative-strand template via a mechanism termed leader-primed transcription (3, 13, 15, 24). UV inactivation studies (8) demonstrated that the subgenomic mRNAs were derived not by cleavage from a large precursor but by independent initiation, on either genome-length or subgenome-length negative-strand templates. Because only genome-length negative-strand templates were found in mouse hepatitis virus (MHV)-infected cells and in replicative intermediates (RIs) obtained from MHV-infected cells and because only genome-length replicative-form (RF) RNA was found in cells infected with MHV (3, 14), it was believed that the leader RNA was copied from the 3′ end of the negative-strand template and was translocated to the intergenic regions that are located upstream of each of the sequences encoding the individual subgenomic mRNAs (6). An alternative model proposed that the negative-strand template looped out to allow the polymerase to skip the sequences between the end of the leader and the beginning of each gene (24). This model was ruled out, because only genome-length RNase-resistant RF RNA was found in cells infected with MHV (3, 14).

The first report that coronaviruses may utilize a subgenome-length negative strand as a template for the synthesis of subgenomic mRNAs was published recently by the laboratory of David Brian at the University of Tennessee (21). They reported that, in cells infected with porcine transmissible gastroenteritis virus, they found subgenome-length negative strands that corresponded to the lengths of the various subgenomic mRNAs. We report here that RIs and RF RNAs that would contain subgenomic negative-strand templates were detected also in MHV-infected cells and that these subgenomic replicative structures were active in RNA synthesis. We used the alphavirus Semliki Forest virus (SFV), which generates only one subgenomic mRNA via internal initiation on genome-length negative-strand templates (for reviews, see references 9 and 25), as a contrasting system to demonstrate the specific production of subgenomic RIs and RF RNAs by MHV. Thus, the identification of subgenomic negative-strand templates in cells infected with MHV suggests a replication strategy that is probably common to all coronaviruses and that would be unique among the single-stranded-RNA animal viruses.

MATERIALS AND METHODS

Cells and viruses. Seventeen clone one (17CL1) mouse cells and the A59 strain of MHV were grown as described previously (19). SFV was grown as described previously (20), and titers were determined by plaque assay on monolayers of 17CL1 cells overlaid with medium containing 0.1% Gelrite (Kelco, San Diego, Calif.) in 60-mm petri dishes.

Radiolabeling and isolation of viral RNAs. 17CL1 cells in 35- or 60-mm petri dishes were infected with MHV or SFV at a multiplicity of infection (MOI) of 20 or 300 PFU per cell. After the adsorption period, the infected cells were fed with Dulbecco modified Eagle medium (pH 6.8) (19) supplemented with 2% fetal bovine serum. The cells were labeled

* Corresponding author.

Downloaded from http://jvi.asm.org/ on March 17, 2020 by guest

with the same medium containing 2% fetal bovine serum, [^{3}H]uridine (34 Ci/mol; ICN Radiochemicals, Irvine, Calif.), and 20 μg of dactinomycin (a generous gift of Merck Sharp & Dohme, West Point, Pa.) per ml, as described below. At the end of the labeling period, the monolayers were washed twice with ice-cold phosphate-buffered saline and solubilized at 2.5×10^6 cells per ml with LET buffer (0.1 M LiCl, 0.01 M Tris hydrochloride [pH 7.4], 0.002 M EDTA) containing 50 mg of lithium dodecyl sulfate per ml and 200 μg of proteinase K per ml. The solubilized cells were passed through a 27-gauge needle to shear the DNA and the RNA was analyzed directly by electrophoresis in agarose gels, or the cells were extracted with phenol and chloroform and the nucleic acid was collected by ethanol precipitation.

Preparation of viral RF RNAs and analysis by gel electrophoresis. The ethanol-precipitated extracts of infected cells were dissolved in deionized water (2.5×10^4 cells per μl) and treated with DNase I (0.5 U/μl; RNase free; Boehringer Mannheim Biochemicals, Indianapolis, Ind.) in 100 mM NaCl–10 mM Tris hydrochloride [pH 7.8]–2 mM $CaCl_2$–2 mM $MgCl_2$ for 15 min at 30°C. When necessary, the extracts were also treated with RNase A (5× crystallized; concentrations varied as described below; Sigma Chemical Co., St. Louis, Mo.) by the addition of a one-third volume of 3× RNase buffer (700 mM NaCl, 10 mM Tris hydrochloride [pH 7.4], 30 mM EDTA) containing RNase A and were incubated for an additional 15 min at 30°C. For analysis on horizontal 0.8% agarose gels submerged in TBE (89 mM Tris, 89 mM boric acid, 2 mM EDTA), 4 μl (RNA from 10^5 cells) of sample was treated first with DNase I (in 8 μl) and then with RNase A (in 12 μl). Proteinase K (5 mg/ml) in lithium dodecyl sulfate (10%) was added (2 μl). After the samples were incubated for 15 min at 30°C, 6 μl of TBE-dye solution (1 part 10× dye in 60% sucrose and 2 parts 5× TBE) was added. The total sample (20 μl) was loaded onto 0.8% agarose gels in TBE (TBE with 0.2% sodium dodecyl sulfate was the running buffer) for 400 V · h or until the bromphenol blue dye was at the end of the gel. If appropriate, the gels were stained with ethidium bromide or were directly processed for fluorography by being soaked in several methanol washes, in methanol containing 1% PPO (2,5-diphenyloxazole), and then in water. The gels were dried under a vacuum before exposure to X-ray film at −80°C. When analyzed on 0.8% agarose gels in MOPS (morpholinepropanesulfonic acid) and formaldehyde, the gel contained 2.2 M formaldehyde in MOPS buffer (10 mM MOPS [pH 7], 5 mM sodium acetate, 1 mM EDTA). The samples were adjusted to 2.2 M formaldehyde–50% formamide in MOPS buffer before electrophoresis. Low-melting-temperature agarose (SeaPlaque; FMC Bioproducts, Rockland, Maine) was used in TBE. To extract the RNA from the gel, a section of the gel was excised with a razor blade and transferred to a tube containing 5 volumes of LET buffer. The sample was heated to 70°C for 5 min and phenol and chloroform extracted. The RNA was ethanol precipitated.

RESULTS

Kinetics of MHV RNA synthesis. Figure 1A shows the kinetics of viral RNA synthesis produced by 17CL1 cells infected with MHV and SFV at different MOI, and Fig. 1B shows the agarose gel analysis of the products of transcription at 5 to 6 or 4 to 5 h postinfection (p.i.), respectively. To eliminate the possibility that subgenomic MHV replicative structures, if detected, were derived from deletion variants, we prepared a stock of virus that was derived from one plaque which was amplified by one passage at a low (<1 PFU per cell) MOI. When assayed at multiplicities sufficient to infect all cells in the culture synchronously, i.e., an MOI of 20 or more, viral RNA synthesis was detectable by 3 h p.i., increased exponentially for the next 2 to 3 h, and continued at a more or less linear rate for at least another 3 to 4 h (Fig. 1A). Infection at an MOI of 20 PFU per cell gave the same kinetics for viral RNA synthesis as infection with 300 PFU per cell, except that at 300 PFU per cell, viral RNA synthesis began 30 to 60 min sooner. Analysis (Fig. 1B) of the products of transcription indicated that genomic and subgenomic single-stranded MHV RNAs were synthesized in the expected ratios; synthesis of RNA-1 and RNA-7 predominated, but RNA-2, RNA-3, RNA-4, RNA-5, and RNA-6 were also detected. No evidence was found for the presence of defective interfering particles in this stock of MHV, even when the stock was used undiluted, e.g., at 300 PFU per cell. There was neither an inhibition of synthesis of the genomic or the subgenomic mRNAs nor extra radiolabeled bands on the gel at 300 PFU per cell that did not appear at 20 PFU per cell. We used an MOI of 20 PFU per cell for the remainder of the experiments. Analysis of SFV transcription was included in this study, because SFV transcribes both genomic and subgenomic mRNA from a genome-length negative strand. Since alphavirus transcription has been well characterized, it provided a reference for comparison with the results obtained for MHV transcription. Infection of 17CL1 cells with SFV produced approximately the same kinetics of viral RNA synthesis as did MHV, except that SFV RNA synthesis was detected an hour

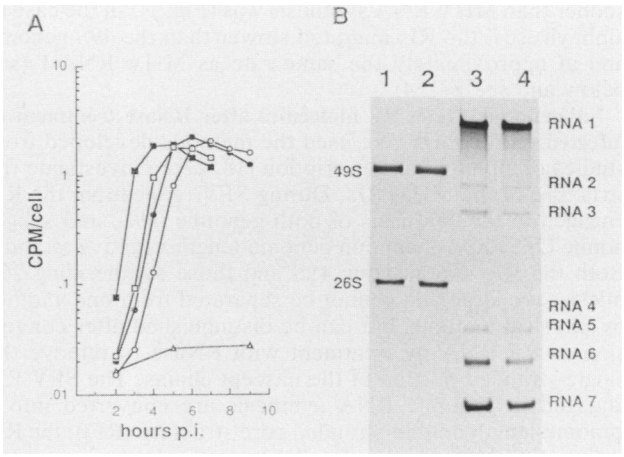

FIG. 1. Effects of MOI on the kinetics of MHV and SFV RNA synthesis at 37°C in 17CL1 cells. A total of 1.4×10^6 17CL1 cells in 35-mm petri dishes were infected with 20 or 300 PFU of MHV or SFV per cell. (A) At hourly intervals after infection, the cells were labeled for 1 h with 50 μCi of [^{3}H]uridine per ml. Duplicate samples of 5×10^4 cells were acid precipitated, and the precipitates were collected on glass fiber filters before the radioactivity was determined by liquid scintillation spectroscopy. Symbols: ○, MHV at 20 PFU per cell; ●, MHV at 300 PFU per cell; □, SFV at 20 PFU per cell; ■, SFV at 300 PFU per cell; △, mock-infected cells. (B) The SFV-infected cells labeled 4 to 5 h p.i. and the MHV-infected cells labeled 5 to 6 h p.i. (the times when viral RNA synthesis reached a maximum rate) were phenol and chloroform extracted and ethanol precipitated. Samples containing 10^5 cells were subjected to electrophoresis in 0.8% agarose–MOPS–formaldehyde gels. Lanes 1 and 2, SFV-infected cells at 300 and 20 PFU per cell, respectively; lanes 3 and 4, MHV-infected cells at 300 and 20 PFU per cell, respectively.

Downloaded from http://jvi.asm.org/ on March 17, 2020 by guest

sooner than MHV RNA synthesis was (Fig. 1). In the case of alphaviruses, the RIs migrated slower than the 49S genome and at approximately the same rate as MHV RNA-1 (see below and see Fig. 4).

Subgenomic MHV RF molecules after RNase treatment of infected cell extracts. We used the methods developed from studies of alphavirus transcription (18, 22) to investigate the structure of the MHV RIs. During SFV replication, the RIs engaged in the synthesis of both genomic (49S) and subgenomic (26S) RNAs contain genome-length negative strands. Both the RIs synthesizing 49S and those synthesizing 26S mRNA are large and cannot be separated from one another by physical methods but can be distinguished after conversion to RF RNA by treatment with RNase to remove the single-stranded portion of the nascent chains. The SFV RIs engaged in genomic RNA synthesis are converted into a genome-length double-stranded core structure (RF_I); the RIs engaged in 26S subgenomic RNA synthesis are converted into two double-stranded cores (the RF_{II} and RF_{III} molecules) by the further cleavage of the negative-strand template in the RIs. RF_{II} represents the 5′ two-thirds of the RF_I molecule, and RF_{III} represents the 3′ one-third and contains sequences encoding the subgenomic 26S mRNA. Presumably, cleavage of the template occurs near the initiation site for transcription of the subgenomic mRNA on the 49S negative strand. We found that RNase concentrations of 1 ng/ml to 33 μg/ml in a buffer containing 0.3 M NaCl caused the production of the three RF cores from the RIs of SFV synthesized in 17CL1 cells (data not shown; see Fig. 3 and 4).

To see whether MHV also caused the production of subgenome-length RF RNA, MHV-infected cells were labeled with [^{3}H]uridine in the presence of dactinomycin from 1 to 6 h p.i., conditions which would maximally label both the negative and positive strands of the MHV RIs (19), and were treated with RNase A under the conditions developed to produce SFV RF RNA. At 6 h p.i., the cells were solubilized with lithium dodecyl sulfate and proteinase K, phenol and chloroform extracted, and ethanol precipitated. Figure 2 shows an autoradiogram of the gel of the labeled products. The extracts applied to lane 1 (Fig. 2) were not treated with DNase I, whereas the extracts applied to the other lanes were treated with DNase I. The 60S MHV genome RNA (RNA-1) comigrated with the cellular DNA which was visualized by staining the gel with ethidium bromide before fluorography. RNA-4 migrated at approximately the same rate as 28S rRNA, and RNA-7, the smallest and most abundant species of MHV single-stranded RNA, migrated faster than the 18S rRNA. Treatment of the extracts with both low (0.1 ng/ml) and high (1 μg/ml) concentrations of RNase A allowed the detection of [^{3}H]uridine-labeled double-stranded MHV RNA, i.e., material resistant to RNase A treatment that migrated as seven distinct bands on the gel. The slowest-migrating RF RNA band (RF_I) had the same mobility as MHV RNA-1. The fastest-migrating RF RNA band (RF_{VII}) had a mobility similar to those of MHV RNA-4 and 28S rRNA. The relative amount of [^{3}H]uridine incorporated into each of the double-stranded RF RNAs reflected the relative amount of [^{3}H]uridine incorporated into each of the single-stranded species of MHV RNA; i.e., the fastest- and slowest-migrating RF RNAs incorporated the most [^{3}H]uridine, which suggested that the fastest-migrating double-stranded RNA was RF_{VII}, the RF of the RI responsible for RNA-7 synthesis, and that the slowest-migrating double-stranded RNA was RF_I, the RF of the RI responsible for RNA-1 synthesis. Since the same amount of cell extract (approximately 10^5 cells) was applied to each lane, a comparison of the intensity of label in the double-stranded RNA bands with that in the single-stranded RNA bands indicated that at least 10 times more label accumulated in the single-stranded RNA species than in the RF RNAs.

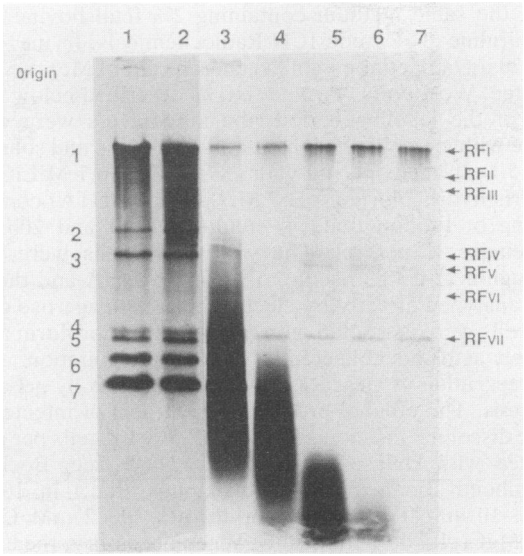

FIG. 2. Effects of DNase and RNase on MHV RNA synthesized between 1 and 6 h p.i. A total of 1.5×10^6 17CL1 cells in a 35-mm petri dish were infected with MHV at 20 PFU per cell and incubated with 100 μCi of [^{3}H]uridine per ml from 1 to 6 h p.i., which maximally labeled both negative and positive strands in the RIs (19). The cells were solubilized, phenol and chloroform extracted, and ethanol precipitated. Lane 1, Untreated; lanes 2 through 7, treated with DNase; lanes 3 through 7, treated with DNase and with RNase A at 0.03 ng/ml (lane 3), 0.33 ng/ml (lane 4), 3.3 ng/ml (lane 5), 33 ng/ml (lane 6), and 333 ng/ml (lane 7). The gel was 0.8% agarose in TBE. Lanes 1 and 2 were exposed at −80°C for 12 h, and lanes 3 through 7 were exposed for 24 h.

Figure 3A shows a direct comparison of SFV RF RNA and MHV RF RNA generated by treatment with 0.1 and 1.0 μg of RNase A per ml. Figure 3B shows a semilog plot of the relative migration rates of each of the RF RNAs. The sizes of these seven RF RNAs were proportional to the expected sizes of subgenomic negative-strand templates for each of the seven MHV RNAs. The numbers of kilobase pairs (kbp) expected for the subgenomic RF RNA were obtained from the reported sequence lengths of mRNA-2 (9.7 kbp), -6 (2.6 kbp), and -7 (1.9 kbp) (1, 2, 16) and by estimating the lengths of RF_{III}, RF_{IV}, and RF_V RNAs from the resulting curve. The RF RNA for RNA-1 was assumed to be 32.7 kbp on the basis of the data published by Pachuk et al. (17). The nonlinear curve of the migration in gels of double-stranded RNAs corresponded to similar curves reported for the migration of other double-stranded RNAs (5). SFV RF_I (11.8 kbp) migrated between MHV RF_I (32.7 kbp) and RF_{II} (9.7 kbp). SFV RF_{II} (7.6 kbp) migrated slightly faster than MHV RF_{III} (8.0 kbp), and SFV RF_{III} (4.2 kbp) migrated between MHV RF_{III} and RF_{IV} (3.7 kbp). During other experiments, in samples that had not been exposed purposefully to RNase, we noted the appearance of extra labeled bands that migrated like MHV RF_{II} and RF_{III} in an area of the gel that had little background (data not shown). Thus, MHV RF_I could be mistaken easily for RNA-1, and MHV RF_{II} and RF_{III} could be interpreted as extra species of single-stranded subgenomic RNA.

Downloaded from http://jvi.asm.org/ on March 17, 2020 by guest

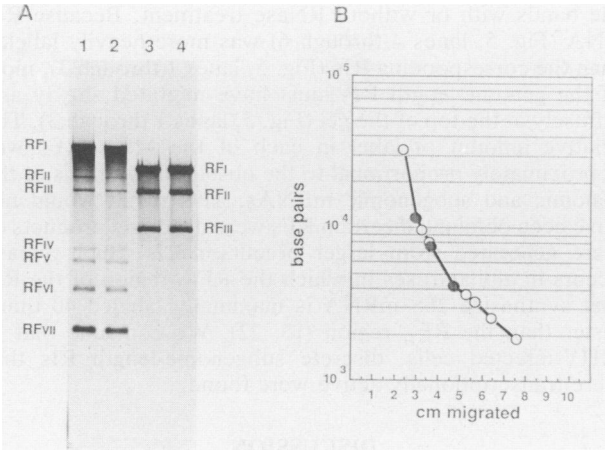

FIG. 3. Sizes of MHV RF RNAs compared with those of SFV RF RNAs. SFV- and MHV-infected cells were labeled 1 to 5 and 1 to 6 h p.i., respectively, with 100 μCi of [^{3}H]uridine per ml. The deproteinized and ethanol-precipitated extracts were exposed to either 0.1 μg (lanes 1 and 4) or 1.0 μg (lanes 2 and 3) of RNase A per ml and electrophoresed in 0.8% agarose gels in TBE. (A) Fluorogram of the gel. Three times more extract was applied to the MHV lanes (lanes 1 and 2; 10^5 cells) than to the SFV lanes (lanes 3 and 4; 3×10^4 cells). (B) Semilog plot of the mobilities of the RF RNAs. Symbols: ●, mobilities of the three SFV RF RNAs (RF_I, 11.8 kbp; RF_{II}, 7.6 kbp; RF_{III}, 4.2 kbp); ○, mobilities of the seven MHV RF RNAs (RF_I, 32.7 kbp; RF_{II}, 9.7 kbp; RF_{III}, 8.0 kbp; RF_{IV}, 3.7 kbp; RF_V, 3.3 kbp; RF_{VI}, 2.6 kbp; RF_{VII}, 1.9 kbp).

Subgenomic MHV RF RNAs are derived from subgenomic RIs active in RNA synthesis. Are the subgenome-length RF RNAs derived from biologically active subgenome-length RIs? We performed two kinds of experiments to answer this question. First, we asked whether the MHV RIs that generated the different-sized species of RF RNA were the same size, as they are in alphaviruses, or whether they were different sizes. Figure 4 shows the results of an experiment designed to answer this question by determining the size of the MHV RIs that generated the seven RFs when treated with RNase A. [^{3}H]uridine-labeled extracts of cells infected with either MHV or SFV were treated with DNase I and electrophoresed in low-melting-temperature agarose. The gel was stained with ethidium bromide, and three regions of the gel (i.e., region A, containing ethidium bromide-stained material that migrated where uncut DNA migrated; region B, where 8- to 12-kilobase single-stranded RNA would migrate; and region C, 1 cm on either side of the 28S region, that would encompass single-stranded RNAs of about 2 to 8 kb) were excised. The RNA was extracted and either was left untreated or was treated with RNase A before being reelectrophoresed on a second agarose gel. RNA extracted from region A of the SFV gel yielded all three alphavirus RF RNAs—RF_I, RF_{II}, and RF_{III}—when treated with RNase A, which is consistent with the previous observations that alphavirus RIs that are engaged in the synthesis of either 49S genomic RNA or 26S subgenomic RNA contain a full-length negative-strand template (Fig. 4) (9, 18, 25). The small amount of single-stranded RNA (the diffusely migrated radiolabeled material) that was present in the lane that was not treated with RNase A was presumably nascent RNA chains that were released from the RIs during heating to 70°C to melt the agarose. In contrast to SFV, the [^{3}H]uridine-labeled MHV RNA that was eluted from the A region of the gel gave mainly MHV RF_I RNA and some labeled RF_{II} and RF_{III}

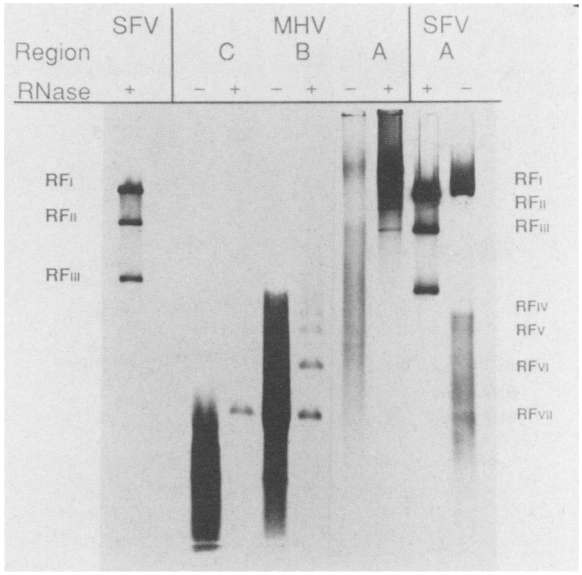

FIG. 4. Subgenome-length MHV RF RNAs generated from subgenome-length RIs. The radiolabeled extracts from 10^6 cells that were infected with MHV or SFV and prepared as described in the legend to Fig. 3 were treated with DNase and electrophoresed in 0.8% low-melting-temperature agarose. The gel was stained with ethidium bromide, and three regions were excised: A, where uncut DNA would have migrated; B, the region about 1 cm above the 28S RNA band and 2 cm below region A; and C, 1 cm on either side of the 28S RNA band. The RNA was then extracted and ethanol precipitated. In the fluorograph, 80% of each sample was treated with 1 μg of RNase A per ml (+), and 20% of each sample was not treated with RNase (−). The samples were electrophoresed on 0.8% agarose in TBE. The leftmost lane is SFV RF RNA used as a reference marker. SFV RF_I, RF_{II}, and RF_{III} were generated by RNase treatment of RNA that migrated in region A. In contrast, only MHV RF_I, RF_{II}, and RF_{III} were generated from region A, while MHV RF_{IV}, RF_V, RF_{VI}, and RF_{VII} were generated from region B but not from region A, and MHV RF_{VII} was generated also from region C.

RNA; no labeled subgenomic RFs of the sizes from RF_{IV} to RF_{VII} were detected. This was not due to lower levels of incorporation of [^{3}H]uridine into the subgenomic RF RNA, because RF_{VII} was as heavily labeled as RF_I (Fig. 3A) and, if present, would have been detected readily. However, labeled RF_{VII} was eluted from the 28S region of the gel (region C) and from the region between 28S rRNA and the MHV RF_{III} RNA (region B). Region B contained, in addition to labeled RF_{VII} RNA, labeled MHV RF_{IV}, RF_V, and RF_{VI} RNAs. MHV RF_{II} and RF_{III} but not RF_I were generated from a region of the gel just below that containing the genomic RNA (data not shown). Thus, the various MHV RF RNAs were generated from a family of RIs that migrated at different rates, which were relative to the sizes expected on the basis of the sizes of their single-stranded products. We conclude that the smaller RF RNAs were not generated by RNase treatment from the same genome-length RIs, as occurs with alphaviruses, but exist in the infected cell as subgenomic replicative structures.

The second approach we used to determine whether RIs smaller than genome length were present in MHV-infected cells and were metabolically active was to employ pulse-labeling conditions to specifically radiolabel structures actively synthesizing MHV RNA. To label the nascent chains

Downloaded from http://jvi.asm.org/ on March 17, 2020 by guest

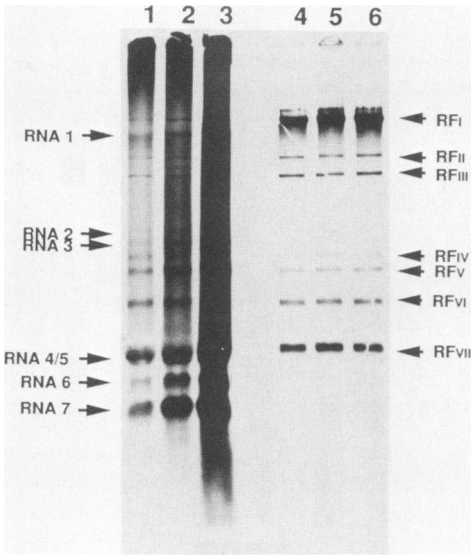

FIG. 5. Transcriptionally active MHV subgenome-length RIs. 17CL1 cells (3×10^6) in 60-mm petri dishes were infected with MHV at 20 PFU per cell and labeled with 1 mCi of [^{3}H]uridine per ml for 2 min (lanes 1 and 4), with 0.25 mCi/ml for 5 min (lanes 2 and 5), or with 0.1 mCi/ml for 20 min (lanes 3 and 6). The cells were solubilized, extracted with phenol and chloroform, and ethanol precipitated. Extracts from 5×10^5 cells were treated with DNase and were either not treated (lanes 1 through 3) or treated (lanes 4 through 6) with 1 μg of RNase A per ml before electrophoresis on an 0.8% agarose gel in TBE.

in MHV RIs, we used pulses of short duration, i.e., 2 to 5 min. Greater amounts of [^{3}H]uridine should be incorporated into the precursor RIs than into the product single strands under these conditions. Figure 5 shows the results of this type of analysis. After a 2-min labeling period, radiolabeled RNA bands corresponding to MHV RNAs RF_I to RF_{VII} were present in the sample that had not been exposed to RNase (Fig. 5, lane 1), and only small amounts of radiolabeled uridine were incorporated into mRNA-6 and mRNA-7, the smallest two subgenomic mRNAs. For very short labeling times, more of the smallest mRNA would be released before much of the largest mRNA would be released, because RNA-7 is about 10 to 15 times shorter and has about 20 times more templates than RNA-1. MHV RNA-7 migrated the fastest as a broad band. By 5 min of pulse-labeling, the larger mRNAs were detectable (Fig. 5, lane 2), and by 20 min (lane 3), most of the label had flowed into single-stranded RNA which obscured detection of the RIs. RNase treatment of the samples unmasked the seven species of RF RNAs (Fig. 5, lanes 4 through 6). All seven species of RFs were labeled in the 2-min pulse, which demonstrated that each of these species was actively engaged in RNA synthesis. Longer pulse periods of 5 to 20 min (Fig. 5) to 300 min (Fig. 2 and 3A) did not alter the relative pattern of incorporation of [^{3}H]uridine into each of the seven RF RNAs, and this pattern was approximately the same as that observed for the synthesis of the product single-stranded mRNAs in infected cells (Fig. 1). RNA-1 migrated faster than MHV RF_I on this type of gel, because extra NaCl was added to the samples not treated with RNase in order to match the concentration of NaCl in the samples treated with RNase. With the exception of the genome-length RIs, labeled RIs (Fig. 5, lanes 1 and 2) migrated at approximately the same rate as the RF RNA, as judged by the intensities of the bands with or without RNase treatment. Because RF_I RNA (Fig. 5, lanes 4 through 6) was more heavily labeled than the corresponding RIs (Fig. 5, lanes 1 through 3), most of the genome-length RIs must have migrated slowly and diffusely at the top of the gel (Fig. 5, lanes 1 through 3). The relative amount of label in each of the MHV RFs was approximately proportional to the observed synthesis of the genomic and subgenomic mRNAs. This result would not have been obtained if certain RFs were dead-end products or were generated from larger precursor RIs. Such a case occurs in alphaviruses in which the RF_{III} region of the RIs that synthesize 26S mRNA is maximally labeled 40 times faster than the RF_{II} region (18, 22). We conclude that in MHV-infected cells, discrete subgenome-length RIs that were transcriptionally active were found.

DISCUSSION

The results show that transcriptionally active subgenome-length RIs accumulate in MHV-infected 17CL1 cells and that the MHV RIs can be converted to seven discrete RFs by treatment with RNase A. Although we have not demonstrated directly that the subgenomic RIs and RFs contained negative strands, we believe that our results strongly support the concept that coronaviruses produce subgenome-length negative strands that are engaged in positive-strand synthesis. Our results corroborate those of Sethna et al. (21), who demonstrated directly that subgenome-length negative strands were present in cells infected with porcine transmissible gastroenteritis virus. Our results contradict those published by Lai et al. (14) and Baric et al. (3), who found only genome-length negative strands in MHV-infected cells. We have no explanation for the failure of Lai et al. (14) to detect the subgenomic negative strands, especially those that corresponded to RNA-7. In our experiments, RF_{VII} appeared to be present in higher molar amounts than RF_I and should have been detected by the procedures used by those authors, which involved probing with radiolabeled positive-strand RNA after Northern (RNA) blotting. Furthermore, because RNA-7 is much smaller, it should have been transferred from the gel at a much higher efficiency than RNA-1. Interestingly, Lai et al. (14) indicated that on occasion, small amounts of radioactive probe hybridized to material that ran near the bottom of their gels. In the case of Baric et al. (3), the RIs were subjected to exclusion chromatography before the sizes of the negative strands associated with the RIs were examined, and this procedure may have eliminated the smaller RIs, especially RI_{VII}, which would elute later than RI_I.

We were able to demonstrate directly that SFV (an alphavirus) and MHV (a coronavirus) use different strategies to produce subgenomic mRNAs in 17CL1 cells. Alphaviruses use full-length negative strands to synthesize both genomic and subgenomic mRNAs (9, 18, 22, 25). Only genome-length negative-strand RNAs are present in alphavirus RIs. The alphavirus RIs sediment at about 20S to 35S on sucrose gradients (18, 22) and migrate in agarose gels more slowly than the 49S genomic RNA. When treated with RNase, alphavirus RIs yield three RFs, which demonstrates that genome-length negative-strand templates are used to produce both genomic and subgenomic mRNAs. A similar strategy for the production of subgenomic mRNA from genome-length negative strands exists in positive-stranded plant viruses (7). There has been no experimental support obtained for the notion that alphavirus RF_{II} (22) or the plant virus RFs (7) result from the association of previously

Downloaded from http://jvi.asm.org/ on March 17, 2020 by guest

released plus strands with the complementary negative-strand sequences as a result of extraction and purification procedures. This is especially the case when short pulse-labels are used to monitor transcriptionally active RIs, since the overwhelming majority of free single-stranded RNAs available for such association would be unlabeled. If internal initiation on negative strands of genome length were employed by coronaviruses for subgenomic mRNA synthesis, seven RFs would be generated by RNase treatment of RIs containing genome-length negative strands. In addition to the RFs corresponding to the subgenomic mRNAs, other species of RFs corresponding to the remaining portions of the genome-length negative strands would also be expected to be generated by RNase treatment. In contrast to SFV RIs, when the largest MHV RIs which would be expected to contain genome-length negative strands were treated with RNase, only genome-length RF_I was generated. Six subgenome-length RFs which were proportional to the subgenomic mRNAs were generated only from subgenomic RIs. Furthermore, we did not find additional species of RFs that would be comparable to RF_{II} of alphaviruses. Therefore, the recently proposed (10) coronavirus "pausing" model for positive-strand synthesis on a genome-length negative-strand template, which is reminiscent of the alphavirus model, is not consistent with our results. We conclude that, unlike alphaviruses, coronaviruses synthesize subgenomic negative strands that serve as templates for the production of subgenomic mRNA.

How do subgenomic negative strands arise and what significance does their presence have for MHV transcription? Sethna et al. (21) hypothesized that their presence indicates that two kinds of subgenomic positive-strand RNA synthesis occur. One kind would utilize the full-length negative strand by the mechanism of leader-primed transcription proposed by Baric et al. (3) and by Spaan et al. (24) or by differential premature termination of transcription (10), which would produce both genomic and subgenomic mRNAs that possess identical 5′ and 3′ ends. These positive-strand molecules then would be copied into the genome- and subgenome-length negative strands. The subgenomic negative-strand templates in turn would be used for a second kind of positive-strand synthesis to amplify the family of subgenomic mRNAs. In this model, subgenomic positive strands would be produced first and would serve as the templates for the generation of subgenomic negative strands; such a model is consistent with the results of UV inactivation studies of positive-strand transcription, which indicate that UV targets are proportional to the size of each of the subgenomic mRNAs (8), and with the results of studies that determined that the 5′ leader sequence on the subgenomic mRNAs was the same as that on the genomic RNA (13, 15, 24). If valid, such a model would also predict that both subgenome- and genome-length RIs would yield subgenomic RFs. We failed to detect subgenomic RFs from genome-length RIs in our analysis. This may be due to the relatively small numbers of genome-length RIs engaged in subgenomic-mRNA synthesis or to the lack of a nuclease-sensitive site in the intergenic regions of the genome-length RIs engaged in subgenomic-mRNA synthesis. Even extensive overexposure of the gel shown in Fig. 4 did not reveal RF_{VII} being generated from RIs containing genome-length templates.

We suggest an alternative model. Subgenomic negative strands are produced directly from genome-length positive strands and are the only templates for subgenomic-mRNA synthesis. Subgenomic negative strands could result from differential premature termination of transcription of the genomic RNA if the intergenic regions functioned as attenuators during the synthesis of negative strands and if negative-strand synthesis terminated at the intergenic regions. In this case, the 3′ ends of the subgenomic negative strands would not encode leader RNA but might include the consensus sequence of the intergenic regions. On the other hand, subgenomic negative strands could result from the looping out of the genomic template during transcription or from the splicing of the nascent negative strand to incorporate in the negative sense the leader sequence encoded at the 5′ end of the genomic RNA (an anti-leader) into each subgenomic negative-strand RNA. All these mechanisms would result in a family of negative-strand templates that would produce a nested set of negative strands; i.e., they would be 5′ coterminal. The major difference between these models is the presence or absence of an anti-leader sequence at the 3′ end of the subgenomic negative strands. Direct sequencing of the 3′ end of the negative-strand templates which would be present in each of the subgenome-length RIs will be necessary to prove that the leader RNA is derived by direct transcription. If the subgenomic negative strands do not contain a sequence complementary to the leader RNA at their 3′ ends, then the subgenomic negative strands would arise by direct transcription of the genome and differential premature termination. If this is found, the leader RNA may be added to each mRNA transcript during an initiation event whereby the polymerase-leader RNA complex would initiate transcription on each of the subgenomic negative strands. Such subgenomic positive-strand synthesis would be similar to that of influenza virus, which also uses a leader-primed mechanism to initiate viral mRNA synthesis but which obtains its leader sequences from the 5′ ends of host cell polymerase II transcripts (for a review, see reference 11). This model would not be inconsistent with the UV sensitivity data for mRNA synthesis obtained by Jacobs et al. (8) and would be compatible with what is known about the presence of a common leader sequence on the coronavirus subgenomic mRNAs.

One more conclusion suggested by our results and those published by Sethna et al. (21) for porcine transmissible gastroenteritis virus was that the relative abundance of each of the subgenomic mRNAs may be determined not by polymerase affinity for the different promoters on the genome-length negative-strand RNA but by the relative abundance of each of the particular negative-strand templates. The relative proportions of incorporation into and accumulation of the MHV RF RNAs were approximately the same as those found for the single-stranded mRNAs. Thus, the relatively large amounts of RNA-1 and RNA-7 mRNAs produced in infected cells correlated with the presence of large numbers of templates for these RNAs. Therefore, transcriptional control would reside at the level of negative-strand synthesis. Whatever the mechanism for generating the subgenomic negative strands, it would govern the amount of each of the seven RIs that accumulate in the infected cell.

Our findings for MHV and those of Sethna et al. (21) for porcine transmissible gastroenteritis virus indicate that probably all coronaviruses utilize the synthesis of subgenomic negative-strand templates to amplify mRNA synthesis. The strategy of producing both genome- and subgenome-length templates for mRNA synthesis suggests that the replication strategy of coronaviruses is novel among the animal RNA viruses and takes advantage of certain aspects of the strategies employed by both positive-strand viruses and segmented negative-strand viruses. The role of the nonstruc-

Downloaded from http://jvi.asm.org/ on March 17, 2020 by guest

tural proteins encoded by the large A gene, estimated at 20 kb for MHV (17) and avian infectious bronchitis virus (4), and by the other nonstructural genes of coronaviruses in the transcriptional processes will undoubtedly be an important and interesting area of study. Our results and those of Sethna et al. (21) strongly suggest that the currently accepted models of MHV transcription need to be reexamined.

ACKNOWLEDGMENTS

This investigation was supported by Public Health Service grants AI-15123 from the National Institute of Allergy and Infectious Diseases and 2SO7-RR05700 for biomedical research support from the National Institutes of Health.

LITERATURE CITED

1. **Armstrong, J., S. Smeekens, and P. Rottier.** 1983. Sequence of the nucleocapsid gene from murine coronavirus MHV-A59. Nucleic Acids Res. **11**:883–891.
2. **Armstrong, J., S. Smeekens, and P. Rottier.** 1984. Sequence and topology of a model intracellular membrane protein, E1 glycoprotein, from a coronavirus. Nature (London) **308**:751–752.
3. **Baric, R. S., S. A. Stohlman, and M. M. C. Lai.** 1983. Characterization of replicative intermediate RNA of mouse hepatitis virus: presence of leader RNA sequences on nascent chains. J. Virol. **48**:633–640.
4. **Boursnell, M. E. G., T. D. K. Brown, I. J. Foulds, P. F. Green, F. M. Tomley, and M. M. Binns.** 1987. Completion of the sequence of the genome of the coronavirus avian infectious bronchitis virus. J. Gen. Virol. **68**:57–77.
5. **Bozarth, R. F., and E. H. Harley.** 1976. The electrophoretic mobility of double-stranded RNA in polyacrylamide gels as a function of molecular weight. Biochim. Biophys. Acta **432**: 329–335.
6. **Budzilowicz, C. J., S. P. Wilczynski, and S. R. Weiss.** 1985. Three intergenic regions of coronavirus mouse hepatitis virus strain A59 genome RNA contain a common nucleotide sequence that is homologous to the 3′ end of the viral mRNA leader sequence. J. Virol. **53**:834–840.
7. **Gargouri, R., R. L. Joshi, J. F. Bol, S. Astier-Manifacier, and A.-L. Haenni.** 1989. Mechanism of synthesis of turnip yellow mosaic virus coat protein subgenomic RNA *in vitro*. Virology **171**:386–393.
8. **Jacobs, L., W. J. M. Spaan, M. C. Horzinek, and B. A. Van Der Zeijst.** 1981. Synthesis of subgenomic mRNAs of mouse hepatitis virus is initiated independently: evidence from UV transcription mapping. J. Virol. **39**:401–406.
9. **Kaariainen, L., K. Takkinen, S. Keranen, and H. Soderlund.** 1987. Replication of the genome of alphaviruses. J. Cell Sci. **7**(Suppl.):231–250.
10. **Konings, D. A. M., P. J. Bredenbeec, J. F. H. Noten, P. Hogeweg, and W. J. M. Spaan.** 1988. Differential premature termination of transcription as a proposed mechanism for the regulation of coronavirus gene expression. Nucleic Acids Res. **16**:10849–10860.
11. **Krug, R. M.** 1985. The role of RNA priming in viral and trypanosomal mRNA synthesis. Cell **41**:651–652.
12. **Lai, M. M. C.** 1988. Replication of coronavirus RNA, p. 115–136. *In* E. Domingo, J. J. Holland, and P. Ahlquist (ed.), RNA genetics, vol. 1. RNA-directed virus replication. CRC Press, Inc., Boca Raton, Fla.
13. **Lai, M. M. C., R. S. Baric, P. R. Brayton, and S. A. Stohlman.** 1984. Characterization of leader RNA sequences on the virion and mRNAs of mouse hepatitis virus, a cytoplasmic RNA virus. Proc. Natl. Acad. Sci. USA **81**:3626–3630.
14. **Lai, M. M. C., C. D. Patton, and S. A. Stohlman.** 1982. Replication of mouse hepatitis virus: negative-stranded RNA and replicative form RNA are of genome length. J. Virol. **44**:487–492.
15. **Lai, M. M. C., C. D. Patton, and S. A. Stohlman.** 1983. Presence of leader sequences in the mRNA of mouse hepatitis virus. J. Virol. **46**:1027–1033.
16. **Luytjes, W., P. J. Bredenbeek, A. F. Noten, M. C. Horzinek, and W. J. Spaan.** 1988. Sequence of mouse hepatitis virus A59 mRNA 2: indications for RNA-recombination between coronaviruses and influenza C virus. Virology **166**:415–422.
17. **Pachuk, C. J., P. J. Bredenbeck, P. W. Zoltick, W. J. M. Spaan, and S. R. Weiss.** 1989. Molecular cloning of the gene encoding the putative polymerase of mouse hepatitis coronavirus, strain A59. Virology **171**:141–148.
18. **Sawicki, D. L., L. Kaariainen, C. Lambek, and P. J. Gomatos.** 1978. Mechanism for control of synthesis of Semliki Forest virus 26S and 42S RNA. J. Virol. **25**:19–27.
19. **Sawicki, S. G., and D. L. Sawicki.** 1986. Coronavirus minus-strand RNA synthesis and effect of cycloheximide on coronavirus RNA synthesis. J. Virol. **57**:328–334.
20. **Sawicki, S. G., and D. L. Sawicki.** 1986. The effect of overproduction of nonstructural proteins on alphavirus plus-strand and minus-strand RNA synthesis. Virology **152**:507–512.
21. **Sethna, P. B., S.-L. Hung, and D. A. Brian.** 1989. Coronavirus subgenomic minus-strand RNAs and the potential for mRNA replicons. Proc. Natl. Acad. Sci. USA **86**:5626–5630.
22. **Simmons, D. T., and J. H. Strauss.** 1972. Replication of Sindbis virus II: multiple forms of double-stranded RNA isolated from infected cells. J. Mol. Biol. **71**:615–631.
23. **Spaan, W., D. Cavanagh, and M. C. Horzinek.** 1988. Coronaviruses: structure and genome expression. J. Gen. Virol. **69**: 2939–2952.
24. **Spaan, W., H. Delius, M. Skinner, J. Armstrong, P. Rottier, S. Smeekens, B. A. van der Ziejst, and S. G. Siddell.** 1983. Coronavirus mRNA synthesis involves fusion of non-contiguous sequences. EMBO J. **2**:1839–1844.
25. **Strauss, J. H., and E. G. Strauss.** 1988. Replication of the RNAs of alphaviruses and flaviviruses. *In* E. Domingo, J. J. Holland, and P. Ahlquist (ed), RNA genetics, vol. 1. RNA-directed virus replication. CRC Press, Inc., Boca Raton, Fla.

Downloaded from http://jvi.asm.org/ on March 17, 2020 by guest